Report

Current Biology

Slower Binocular Rivalry in the Autistic Brain

Highlights

- Binocular rivalry is slower in the autistic brain
- Potential marker of E/I balance in visual cortex
- Predicts clinical symptoms and classifies diagnostic status (autism versus controls)
- Non-verbal measure, which may be suitable for infant and cross-species research

Authors

Alina Spiegel, Jeff Mentch, Amanda J. Haskins, Caroline E. Robertson

Correspondence

caroline.e.robertson@dartmouth.edu

In Brief

Robertson et al. report that a basic visual phenomenon, binocular rivalry, is altered in the autistic brain. This result firmly implicates the visual cortex in the neurobiology of autism and may reflect an imbalance in E/I neurotransmission. As a non-verbal paradigm, this marker of autism may be suitable for future infant and cross-species studies.

Spiegel et al., 2019, Current Biology *29*, 2948–2953
September 9, 2019
https://doi.org/10.1016/j.cub.2019.07.026

CellPress

CellPress

Current Biology
Report

Slower Binocular Rivalry in the Autistic Brain

Alina Spiegel,[1] Jeff Mentch,[2,3] Amanda J. Haskins,[2] and Caroline E. Robertson[2,4,*]
[1]School of Medicine, Johns Hopkins University, Baltimore, MD 21205, USA
[2]Department of Psychological and Brain Sciences, Dartmouth College, Hanover, NH 03755, USA
[3]Department of Brain and Cognitive Sciences, Massachusetts Institute of Technology, Cambridge, MA 02139, USA
[4]Lead Contact
*Correspondence: caroline.e.robertson@dartmouth.edu
https://doi.org/10.1016/j.cub.2019.07.026

SUMMARY

Autism has traditionally been regarded as a disorder of the social brain. Recent reports of differences in visual perception have challenged this notion, but little evidence for altered visual processing in the autistic brain exists. We have previously observed slower behaviorally reported rates of a basic visual phenomenon, binocular rivalry, in autism [1, 2]. During rivalry, two images—one presented to each eye—vie for awareness, alternating back and forth in perception. This competition is modeled to rely, in part, on the balance of excitation and inhibition in visual cortex [3–8], which may be altered in autism [2, 9–14]. Yet direct neural evidence for this potential marker of excitation/inhibition (E/I) balance in autism is lacking. Here, we report a striking alteration in the neural dynamics of binocular rivalry in individuals with autism. Participants viewed true and simulated frequency-tagged binocular rivalry displays while steady-state visually evoked potentials (SSVEPs) were measured over occipital cortex using electroencephalography (EEG). First, we replicate our prior behavioral findings of slower rivalry and reduced perceptual suppression in individuals with autism compared with controls. Second, we provide direct neural evidence for slower rivalry in autism compared with controls, which strongly predicted individuals' behavioral switch rates. Finally, using neural data alone, we were able to predict autism symptom severity (ADOS) and correctly classify individuals' diagnostic status (autistic versus control; 87% accuracy). These findings clearly implicate atypical visual processing in the neurobiology of autism. Down the road, this paradigm may serve as a non-verbal marker of autism for developmental and cross-species research.

RESULTS AND DISCUSSION

Thirty-seven adult participants (18 autism and 19 age- and IQ-matched controls; Table S1) viewed true and simulated frequency-tagged binocular rivalry displays while steady-state visually evoked potentials (SSVEPs) were measured over occipital cortex using electroencephalography (EEG) (Figure 1A). During rivalry, activity levels in neuronal populations coding for left- and right-eye percepts rise and fall in alternation as the two images fluctuate in perceptual awareness [15]. We first sought to identify this counterphase neural activity associated with rivalry in the human brain using EEG. To independently track the ebb and flow of neural activity corresponding to each eye during rivalry, we tagged the two images presented to each eye with a signature frequency (5.67 or 8.5 Hz) and measured activity in the two corresponding frequency bands over time (Figures 1A and S1) [16, 17]. As predicted, left- and right-eye signals fluctuated in counterphase during both rivalry trials (Figures 1B, 2A, and 2B) and control rivalry simulation trials (Figures 3A and 3B): as one eye's signal increased, the other eye's signal decreased.

To quantify this counterphase relationship between left- and right-eye signals, we calculated the mean phase-locking values (PLVs) between the power in the left- and right-eye frequency bands, where a 0-degree PLV indicates perfectly in-phase signals and a 180-degree PLV indicates perfectly antiphase signals (Figure 2A). Left- and right-eye signals were significantly antiphase during rivalry trials (controls, top: 207.97° ± 9.18° STE; autism, bottom: 208.74° ± 14.48° STE; difference from 0 degrees: both $p < 0.001$; difference from 180 degrees: both $p > 0.170$; group difference: $p = 0.50$). Rivalry PLVs were also significantly "peaky," or non-uniformly distributed around 180 degrees (Rayleigh test of non-uniformity, controls: $Z = 5.06$, $p < 0.001$; autism: $Z = 9.07$, $p < 0.001$). Further, PLVs during rivalry trials were comparable to those observed during rivalry simulation trials, where two frequency-tagged images were displayed in temporal alternation on the screen and therefore drove known, stimulus-locked antiphase responses (controls, top: 200.48° ± 19.99° STE; autism, bottom: 199.84° ± 13.84° STE; difference from rivalry PLVs: both $p > 0.153$; Figure 3A). In contrast, rivalry PLVs and vector magnitudes were significantly greater than those derived from noise simulations in both groups (both $p < 0.002$), emphasizing that the significant antiphase modulations we observed during rivalry trials are unlikely to occur by chance. These results demonstrate that robust, rivalry-like alternations in left- and right-eye signals were recorded over occipital cortex during our binocular rivalry experiment.

We next developed a metric to quantify individual differences in rivalry alternations from these neurally derived signals. In brief, this Neural Rivalry Index (NRI) determines the characteristic frequency of the alternation in power between left- and right-eye signals during rivalry for each participant

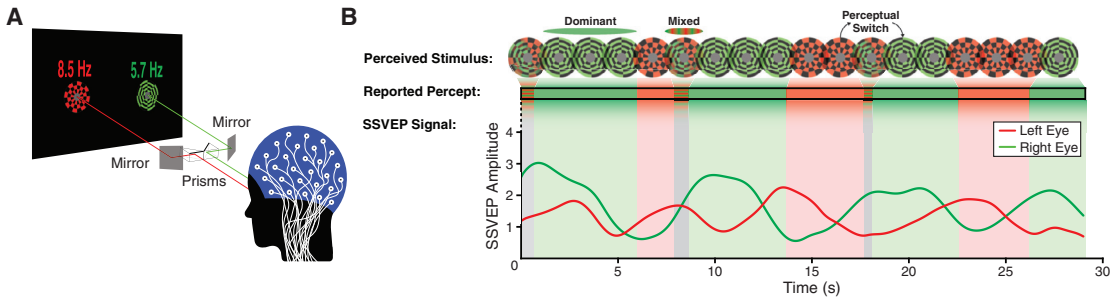

Figure 1. Experimental Paradigm: Neural Measurement of Binocular Rivalry

(A) Participants viewed two frequency-tagged images through a mirror stereoscope, which reflected the left and right sides of the screen to the participant's left and right eyes (respectively) so that each eye viewed a unique image. To independently track the neural response corresponding to each percept in the brain, the two images were tagged with different frequencies (i.e., each image contrast reversed on the screen at either 5.67 or 8.5 Hz) and continuous EEG was recorded from occipital cortex (steady-state visually evoked potentials [SSVEPs]).

(B) Example data from one 30-s rivalry trial. During rivalry, left- and right-eye percepts compete for perceptual dominance, alternating back and forth in awareness (as seen in participant's report, top of panel). Neural data match this reported perceptual alternation (shown in the SSVEP signal, bottom of panel). Power corresponding to the left- or right-eye frequency bands alternates over time (solid lines): as one eye's signal increases, the other eye's signal decreases. This neural rivalry alternation occurs in coordination with individuals' perceptual report over the course of the trial (perceptual report is shaded in background).

(STAR Methods). To validate the NRI metric, we compared individuals' NRIs to behaviorally reported switch rates as well as to known image changes during rivalry simulation trials. The NRI strongly predicted participants' perceptual switch rates in both groups (controls: Pearson's $R = 0.76$, $p < 0.001$; autism: Pearson's $R = 0.54$, $p = 0.020$; group difference $p = 0.27$; Figure 4A) and matched the rate of controlled image changes during rivalry simulation trials (controls: 0.43 ± 0.01 Hz STE; autism: 0.42 ± 0.01 Hz STE; ground truth: 0.5 Hz). NRIs during control trials were slightly slower than the true rate of controlled image changes (controls: $t(18) = -6.97$, $p < 0.01$; autism: $t(17) = -10.72$, $p < 0.01$). However, this loss was equal for the two groups (group difference in simulation NRIs: $F(1,35) = 0.56$; $\eta_p^2 = 0.016$; $p = 0.461$) and therefore unlikely to mediate group differences during rivalry trials. Although rivalry-like alternations have been previously observed in humans using SSVEP [16–18], to our knowledge, these results provide the first neural metric to quantify individual differences in perceptual alternation rates during rivalry.

We next compared the rates of neural rivalry alternations (measured using NRIs) in individuals with and without autism. We observed markedly slower neural binocular rivalry alternations for individuals with autism as compared with controls (controls: 0.40 ± 0.01 Hz STE; autism: 0.35 ± 0.01 Hz STE; group difference: $F(1,35) = 8.399$; $\eta_p^2 = 0.194$; $p = 0.006$; Figures 2B and 2C). This slower rate of rivalry in the autistic brain was directly mirrored in each group's behaviorally reported switch rates, replicating our previous behavioral results of slower rivalry in autism [1, 2, 19]. Specifically, although control individuals reported perceptual switches at 0.35 (switches per second) ± 0.02 Hz STE, switch rates for individuals with autism were nearly 60% of this speed at 0.21 ± 0.02 Hz STE ($F(1,35) = 21.8$; $\eta_p^2 = 0.384$; $p < 0.001$; Figure 2C). Additionally, this slower rate of binocular rivalry in behavior was marked by a reduced proportion of perceptual suppression in individuals with autism (controls: 0.84 ± 0.02 STE; autism: 0.68 ± 0.04 STE; group difference: $F(1,35) = 11.51$; $\eta_p^2 = 0.248$; $p = 0.002$; Figure S2). In contrast, comparable behavioral switch rates were observed during rivalry simulation control trials, indicating comparable task understanding between our two groups ($p = 0.889$; Figure 3C). These results provide a direct neural readout of slower binocular rivalry in individuals with autism, obtained without any need for participant reporting.

This neural marker of slower binocular rivalry dynamics in autism predicted clinical measures of autistic symptomatology. Individuals with slower rivalry dynamics in the brain showed higher autistic symptoms (ADOS social subscale; Rho = −0.48, $p = 0.045$; ADOS total; Rho = −0.44, $p = 0.064$; Figure 4B), although a self-report scale of autistic traits (AQ) did not predict rivalry dynamics in either group (both $p > 0.34$). No relationship was observed between IQ and either neural (both $p > 0.176$) or behavioral switch rates (both $p > 0.127$) in either group, indicating that these effects were independent of individual differences in general intelligence, on which the groups were matched (Table S1). Consistent with our previous findings [1, 2], these results indicate that this relatively low-level perceptual marker of autism is associated with clinically measured autistic traits defined at much more complex levels of behavior.

Crucially, these results could not be explained by group differences in SSVEP signal quality or the duration of general (non-rivalrous) evoked visual responses. First, for both groups, signal was high and significantly greater than noise throughout the experiment for both frequencies (autism 5.67 Hz: $t(17) = 11.03$, $p < 0.001$; autism 8.5 Hz: $t(17) = 10.92$, $p < 0.001$; controls 5.67 Hz: $t(18) = 8.48$, $p < 0.001$; controls 8.5 Hz: $t(18) = 10.14$, $p < 0.001$; 5.67 Hz group difference: $F(1,35) = 0.11$, $\eta_p^2 = 0.003$, $p = 0.742$; 8.5 Hz group difference: $F(1,35) = 3.428$, $\eta_p^2 = 0.089$, $p = 0.073$; Figure S1). Second, the rate of neural alternations (NRIs) during rivalry simulation control trials, where binocularly viewed images were displayed in temporal alternation on the screen, were comparable between individuals with and without autism (controls: 0.43 ± 0.01 Hz STE; autism: 0.42 Hz ± 0.01 Hz STE; group difference: $F(1,35) = 0.555$; $\eta_p^2 = 0.016$; $p = 0.461$; Figures 3B and 3C). Finally, group differences in rivalry NRIs could not reflect group differences in neural signals associated with motor responses, rather than visually evoked responses, as NRIs specifically compare power in the

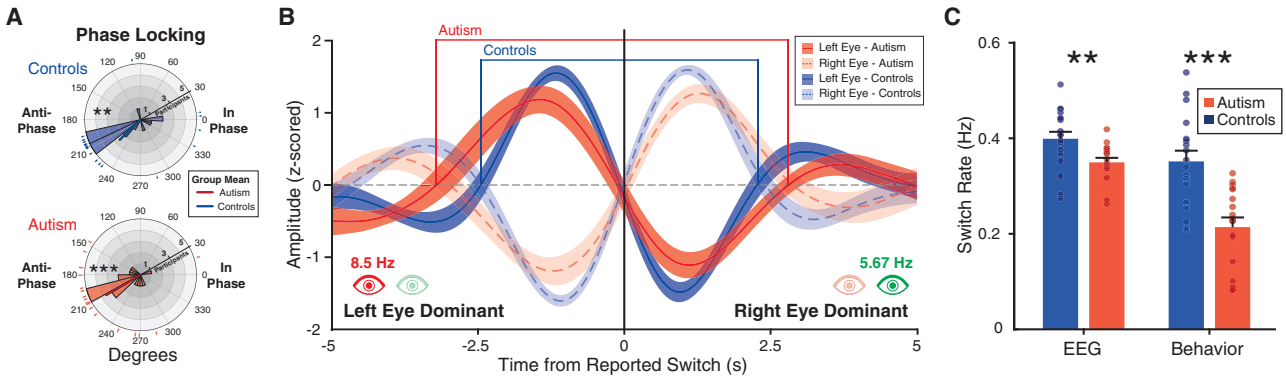

Figure 2. Slower Binocular Rivalry in the Autistic Brain

(A) We observed rivalry-like alternations in neural activity recorded from visual cortex in both individuals with and without autism: as one eye's SSVEP signal increased, the other eye's signal decreased. To quantify this antiphase relationship, we calculated the mean phase-locking values (PLVs) between the power in the left- and right-eye frequency bands (where a 0-degree PLV indicates perfectly in-phase signals and a 180-degree PLV indicates perfectly antiphase signals). Left- and right-eye signals were significantly antiphase during rivalry trials for both groups (both $p < 0.001$), and PLVs were significantly greater than mean PLV magnitudes derived from noise simulations (both $p < 0.002$).

(B) For illustration purposes, left- and right-eye data are averaged ±5 s before and after each reported left-to-right eye perceptual switch for both groups. As can be seen, left- and right-eye signals alternated around the point of a perceptual switch for both groups: left-eye signals (solid lines) rose and fell around each perceptual switch, and right-eye signals (dotted lines) showed the opposite response pattern. Importantly, the average duration of one epoch of binocular rivalry was slower for individuals with autism, as compared with controls, as can be seen by comparing the zero crossings of the two left-eye signals (quantified in C). Shaded region represents ±1 SEM.

(C) To quantify the rate of individual neural rivalry alternations, we calculated the characteristic frequency of rivalry measured from visual cortex (the Neural Rivalry Index [NRI]). The rate of both neural (left) and behavioral (right) binocular rivalry alternations for individuals with autism as compared with controls (both $p < 0.01$) is shown.

In all plots, error bars represent 1 SEM. **$p < 0.01$; ***$p < 0.001$ difference between the two groups. See also Figures S1 and S2 and Table S1.

two visually evoked frequency bands (8.5 Hz and 5.67 Hz) rather than in the much slower frequency bands associated with button-press responses (controls: 0.35 Hz and autism: 0.21 Hz). These results indicate that the slower rate of binocular rivalry we observed in the autistic brain cannot be accounted for by differences in rivalry signal quality, the duration of evoked visual responses to non-rivalrous stimuli, or motor responses between the groups.

Finally, we asked whether our measurements of binocular rivalry dynamics in the autistic brain could accurately classify an individual's diagnostic status using a linear support vector machine classifier. Using a leave-one-out cross-validation procedure with individuals' trial-averaged NRIs and frequency-tagged amplitudes as features, we were able to classify an individual's diagnostic status (autism versus control) with 86.5% accuracy (±0.06 STE; sensitivity = 0.83; specificity = 0.89; $p < 0.001$; Figure 4C). Thus, this basic alteration in the autistic visual cortex is not only correlated with higher-order autistic symptoms in social cognition but also predictive of diagnostic status (autism versus controls). Notably, this accuracy level is comparable to the results of classification analyses using hallmark autistic traits in social behavior, such as eye-to-mouth gaze preferences in toddlers with autism (classification accuracy = 86%) [20].

Our findings demonstrate a slower rate of binocular rivalry in the autistic brain. Importantly, this finding was specific to dichoptic, rivalrous displays, where two images compete for perceptual awareness. In contrast, neural alternations elicited by rivalry simulation trials, where binocularly viewed images were displayed in temporal alternation on the screen, were comparable between groups. This pattern of results underscores that visual processing is not generally altered in autism but perhaps specifically altered by visual processes that tax competitive interactions in visual cortex, such as rivalry [3–8]. In classic models of rivalry, competition is supported by two dynamics: recurrent excitation within the neural population selective for the dominant image and cross-inhibition of the neural population selective for the non-dominant image, both of which adapt over time and recover [3, 21, 22]. For example, rivalry is observed in primary visual cortex, where neurons in left- and right-eye ocular dominance columns interact via lateral inhibition: as left-eye ocular dominance columns become active, right-eye columns are suppressed [15]. A slower rate of rivalry in autism likely reflects an alteration in this competitive neural motif, a motif that is thought to be integral to resolving perceptual ambiguity at multiple levels of the visual hierarchy [23, 24].

Although the precise nature of this alteration is unknown, recent magnetic resonance spectroscopy results suggest that the inhibitory neurotransmitter GABA may play a role [2]. In control individuals, levels of both the inhibitory neurotransmitter (GABA) and the excitatory neurotransmitter (glutamate) predict perceptual suppression during rivalry in control individuals, as consistent with models of rivalry described above [3, 21, 22]. However, the link between GABA and rivalry is specifically absent in autism, in contrast with glutamate, which strongly predicts rivalry dynamics, leading to the hypothesis that GABAergic inhibition may be disrupted in the autistic visual cortex [2]. This observation is consistent with other findings in the magnetic resonance spectroscopy (MRS) literature linking GABA to altered tactile and auditory processing in the condition [25–27], as well as animal-level findings of altered inhibitory signaling in the condition [13, 28].

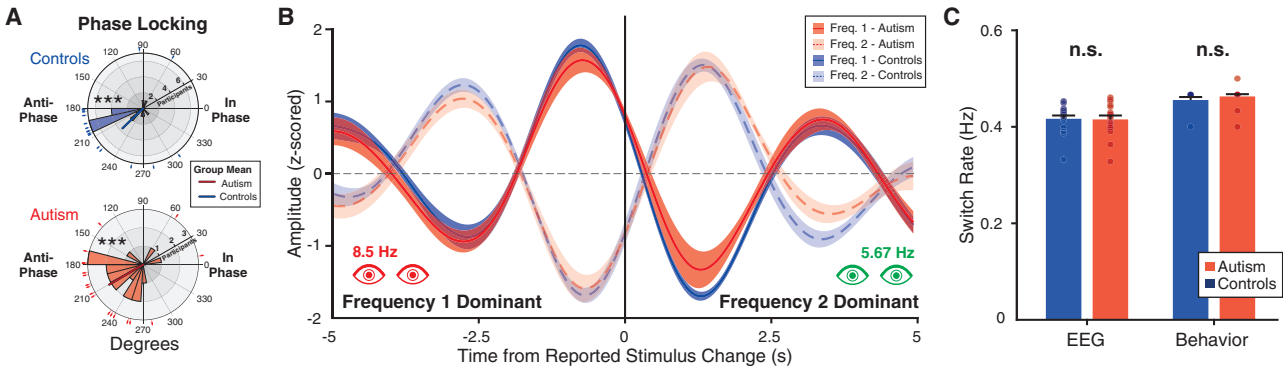

Figure 3. Comparable Visual Responses to Rivalry Simulation Control Trials

(A) During rivalry simulation control trials, both eyes viewed the same frequency-tagged checkerboards at any given time. The two checkerboards, either red (e.g., 8.5 Hz) or green (e.g., 5.67 Hz), alternated back and forth on the screen throughout the duration of the trial. Similar to rivalry, during rivalry simulations, the power in left- and right-eye frequency bands was significantly antiphase throughout simulation trials for both groups (both $p < 0.001$) and PLVs were significantly greater than mean PLV magnitudes derived from noise simulations (both $p < 0.001$).

(B) Data from the two frequency bands are averaged ±5 s before the time when participants' reported the stimulus on the screen changing from a red (8.5 Hz) to a green (5.67 Hz) image, for illustration purposes. For both groups, power in the two frequency bands alternated around the point of a reported switch for both groups, as expected. Shaded region represent ±1 SEM.

(C) Crucially (left), the rate of neural alternations (NRIs) during rivalry simulation control trials were comparable between individuals with and without autism (controls: 0.43 ± 0.01 Hz STE; autism: 0.42 ± 0.01 Hz STE; group difference: $F(1,35) = 0.555$; $\eta_p^2 = 0.016$; $p = 0.461$). Similarly (right), behaviorally reported image changes were comparable between the two groups during rivalry simulation control trials (both $p > 0.89$).

In all plots, error bars represent 1 SEM; n.s., $p > 0.05$; ***$p < 0.001$. See also Figure S1.

Intriguingly, we observed a strong relationship between the neural dynamics of binocular rivalry in autism and clinical measures of high-order autistic symptoms in social behavior. This result highlights the emerging link between perceptual and social autistic traits in the autism literature [29]: perplexingly, laboratory-based measures of perceptual processing in autistic adults routinely predict higher-order symptoms in social and cognitive domains [2, 30–38], an effect that is also observed in population-level studies of self-reported sensory and social traits [39–43]. Why might such a low-level alteration in visual cortex predict high-level symptoms defined in social-cognitive behavior? One possibility is that basic visual functions, like binocular rivalry, rely on canonical neural motifs—divisive normalization, mutual inhibition, and attention [4, 8, 44]—which are ubiquitous in the brain and serve as core computational units for both social and non-social processes [29, 45]. Future work is needed to test this hypothesis.

Our measure of altered rivalry dynamics in autism is entirely non-verbal, derived directly from a neural readout of binocular rivalry alternations in visual cortex and naive to participants' perceptual reports. Further, rivalry alternations covaried with autistic traits, but not general intelligence. As such, this

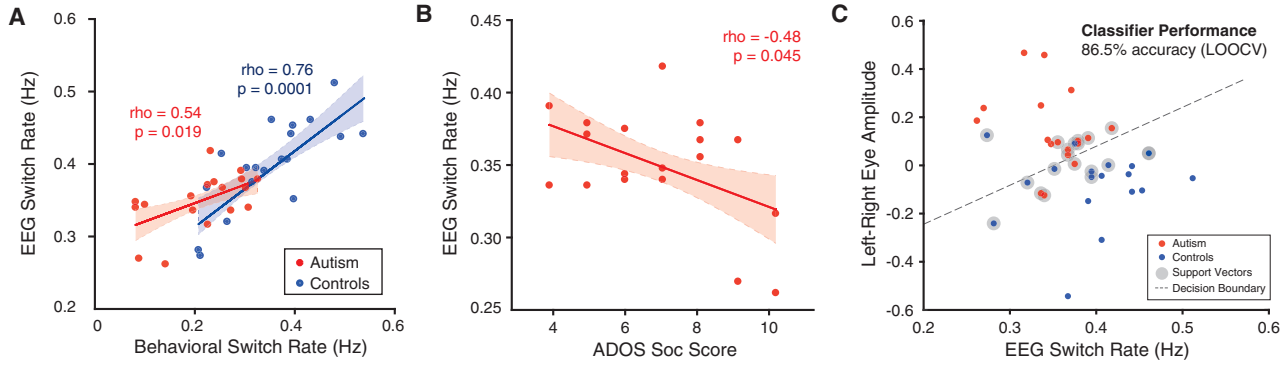

Figure 4. Neural Rivalry Alternations Predict Behavioral Switch Rates, Autistic Traits, and Autism Diagnosis

(A) For each individual, the rate of rivalry alternations measured from visual cortex (NRI) strongly predicted the rate of behaviorally reported rivalry switch rate (controls: rho = 0.76, $p < 0.001$; autism: rho = 0.54, $p < 0.001$). This demonstrates a non-verbal metric for quantifying individual differences in neural rivalry alternations. Shaded regions represent the 95% confidence interval of the regression line.

(B and C) Our neural metric of perceptual alternation rates during binocular rivalry (B) predicted individuals' clinical symptomatology (ADOS scores) and (C) could be used to classify individuals' diagnostic status (autism versus controls) with 86.5% accuracy (±0.06 STE; sensitivity = 83%; specificity = 89%; $p < 0.001$). Overall support vector machine classifier performance was determined using leave-one-out cross-validation (LOOCV). Shaded regions represent the 95% confidence interval of the regression line, and error bars represent 1 SEM. ***$p < 0.001$.

perceptual marker of autism appears well-suited for use in translational cross-species research, as it may index a neural motif that would not be affected by differences in verbal or cognitive abilities across species. Likewise, it may also be well-suited for developmental research with pre-verbal infants. Although electrophysiological signatures of rivalry in infants are to date undocumented [46], some behavioral evidence for rivalry in human infants exists [47] and electrophysiological signatures of interocular suppression are observed by 4 weeks of age in non-human primates [48, 49], suggesting that key anatomical substrates of rivalry are present early in development. A final exciting possibility is that this non-verbal paradigm might be suitable for use with minimally or non-verbal individuals with autism, who are estimated to represent 30% of the autism spectrum but are rarely included in research [50, 51].

All in all, these findings firmly implicate the visual cortex in the neurobiology of autism. Moving forward, it will be important to understand the circuit-level basis of these alterations in binocular rivalry in animal models of autism, as well as their developmental onset in children with autism.

STAR★METHODS

Detailed methods are provided in the online version of this paper and include the following:

- KEY RESOURCES TABLE
- LEAD CONTACT AND MATERIALS AVAILABILITY
- EXPERIMENTAL MODEL AND SUBJECT DETAILS
- METHOD DETAILS
  - Psychometric testing
  - Stimuli and Display
  - Practice, Rivalry, and Rivalry Simulation Trials
  - EEG Data Acquisition and Pre-processing
- QUANTIFICATION AND STATISTICAL ANALYSIS
  - SSVEP Data Analysis: SNR Calculation
  - SSVEP Data Analysis: Extracting Response Amplitude Over Time
  - SSVEP Data Analysis: Antiphase Calculation of Response Amplitude Time courses and Noise Simulations
  - SSVEP Data Analysis: Neural Rivalry Index Calculation
  - SSVEP Data Analysis: Intermodulation Frequencies
  - Support-Vector Machine Analysis: Diagnostic Classification
  - Behavioral Data Analysis
- DATA AND CODE AVAILABILITY

SUPPLEMENTAL INFORMATION

Supplemental Information can be found online at https://doi.org/10.1016/j.cub.2019.07.026.

ACKNOWLEDGMENTS

We thank Jackson Lee and Jan Freyberg for help with data collection and Laura Lewis, Haoran Xu, Brad Duchaine, and Nancy Kanwisher for helpful comments. This work was supported by grants from the MIT-MGH Grand Challenge and the Simons Foundation Autism Research Initiative (SFARI no. 571124) to C.E.R.

AUTHOR CONTRIBUTIONS

Conceptualization, A.S. and C.E.R.; Methodology, A.S., A.J.H., and C.E.R.; Investigation, A.S., J.M., A.J.H., and C.E.R.; Writing – Original Draft, A.S. and C.E.R.; Writing – Review & Editing, A.S., J.M., A.J.H., and C.E.R.; Visualization, J.M.; Funding Acquisition, C.E.R.; Resources, A.J.H. and C.E.R.; Supervision, C.E.R.

DECLARATION OF INTERESTS

The authors declare no competing interests.

Received: March 15, 2019
Revised: May 31, 2019
Accepted: July 10, 2019
Published: August 15, 2019

REFERENCES

1. Robertson, C.E., Kravitz, D.J., Freyberg, J., Baron-Cohen, S., and Baker, C.I. (2013). Slower rate of binocular rivalry in autism. J. Neurosci. *33*, 16983–16991.
2. Robertson, C.E., Ratai, E.-M., and Kanwisher, N. (2016). Reduced GABAergic action in the autistic brain. Curr. Biol. *26*, 80–85.
3. Laing, C.R., and Chow, C.C. (2002). A spiking neuron model for binocular rivalry. J. Comput. Neurosci. *12*, 39–53.
4. Seely, J., and Chow, C.C. (2011). Role of mutual inhibition in binocular rivalry. J. Neurophysiol. *106*, 2136–2150.
5. Said, C.P., and Heeger, D.J. (2013). A model of binocular rivalry and cross-orientation suppression. PLoS Comput. Biol. *9*, e1002991.
6. van Loon, A.M., Knapen, T., Scholte, H.S., St John-Saaltink, E., Donner, T.H., and Lamme, V.A. (2013). GABA shapes the dynamics of bistable perception. Curr. Biol. *23*, 823–827.
7. Noest, A.J., van Ee, R., Nijs, M.M., and van Wezel, R.J.A. (2007). Percept-choice sequences driven by interrupted ambiguous stimuli: a low-level neural model. J. Vis. *7*, 10.
8. Li, H.-H., Rankin, J., Rinzel, J., Carrasco, M., and Heeger, D.J. (2017). Attention model of binocular rivalry. Proc. Natl. Acad. Sci. USA *114*, E6192–E6201.
9. Ma, D.Q., Whitehead, P.L., Menold, M.M., Martin, E.R., Ashley-Koch, A.E., Mei, H., Ritchie, M.D., Delong, G.R., Abramson, R.K., Wright, H.H., et al. (2005). Identification of significant association and gene-gene interaction of GABA receptor subunit genes in autism. Am. J. Hum. Genet. *77*, 377–388.
10. Sanders, S.J., Ercan-Sencicek, A.G., Hus, V., Luo, R., Murtha, M.T., Moreno-De-Luca, D., Chu, S.H., Moreau, M.P., Gupta, A.R., Thomson, S.A., et al. (2011). Multiple recurrent de novo CNVs, including duplications of the 7q11.23 Williams syndrome region, are strongly associated with autism. Neuron *70*, 863–885.
11. Fatemi, S.H., Reutiman, T.J., Folsom, T.D., and Thuras, P. (2009). GABA(A) receptor downregulation in brains of subjects with autism. J. Autism Dev. Disord. *39*, 223–230.
12. Gogolla, N., Takesian, A.E., Feng, G., Fagiolini, M., and Hensch, T.K. (2014). Sensory integration in mouse insular cortex reflects GABA circuit maturation. Neuron *83*, 894–905.
13. Orefice, L.L., Zimmerman, A.L., Chirila, A.M., Sleboda, S.J., Head, J.P., and Ginty, D.D. (2016). Peripheral mechanosensory neuron dysfunction underlies tactile and behavioral deficits in mouse models of ASDs. Cell *166*, 299–313.
14. Marín, O. (2012). Interneuron dysfunction in psychiatric disorders. Nat. Rev. Neurosci. *13*, 107–120.
15. Xu, H., Han, C., Chen, M., Li, P., Zhu, S., Fang, Y., Hu, J., Ma, H., and Lu, H.D. (2016). Rivalry-like neural activity in primary visual cortex in anesthetized monkeys. J. Neurosci. *36*, 3231–3242.
16. Zhang, P., Jamison, K., Engel, S., He, B., and He, S. (2011). Binocular rivalry requires visual attention. Neuron *71*, 362–369.

17. Brown, R.J., and Norcia, A.M. (1997). A method for investigating binocular rivalry in real-time with the steady-state VEP. Vision Res. *37*, 2401–2408.
18. Katyal, S., Vergeer, M., He, S., He, B., and Engel, S.A. (2018). Conflict-sensitive neurons gate interocular suppression in human visual cortex. Sci. Rep. *8*, 1239.
19. Freyberg, J., Robertson, C.E., and Baron-Cohen, S. (2015). Reduced perceptual exclusivity during object and grating rivalry in autism. J. Vis. *15*, 11.
20. Constantino, J.N., Kennon-McGill, S., Weichselbaum, C., Marrus, N., Haider, A., Glowinski, A.L., Gillespie, S., Klaiman, C., Klin, A., and Jones, W. (2017). Infant viewing of social scenes is under genetic control and is atypical in autism. Nature *547*, 340–344.
21. Wilson, H.R., Blake, R., and Lee, S.H. (2001). Dynamics of travelling waves in visual perception. Nature *412*, 907–910.
22. Kang, M.-S., Lee, S.-H., Kim, J., Heeger, D., and Blake, R. (2010). Modulation of spatiotemporal dynamics of binocular rivalry by collinear facilitation and pattern-dependent adaptation. J. Vis. *10*, 3.
23. Wilson, H.R. (2003). Computational evidence for a rivalry hierarchy in vision. Proc. Natl. Acad. Sci. USA *100*, 14499–14503.
24. Tong, F., Nakayama, K., Vaughan, J.T., and Kanwisher, N. (1998). Binocular rivalry and visual awareness in human extrastriate cortex. Neuron *21*, 753–759.
25. Puts, N.A.J., Wodka, E.L., Harris, A.D., Crocetti, D., Tommerdahl, M., Mostofsky, S.H., and Edden, R.A.E. (2017). Reduced GABA and altered somatosensory function in children with autism spectrum disorder. Autism Res. *10*, 608–619.
26. Sapey-Triomphe, L.A., Lamberton, F., Sonié, S., Mattout, J., and Schmitz, C. (2019). Tactile hypersensitivity and GABA concentration in the sensorimotor cortex of adults with autism. Autism Res *12*, 562–575.
27. Gaetz, W., Bloy, L., Wang, D.J., Port, R.G., Blaskey, L., Levy, S.E., and Roberts, T.P.L. (2014). GABA estimation in the brains of children on the autism spectrum: measurement precision and regional cortical variation. Neuroimage *86*, 1–9.
28. Gogolla, N., Leblanc, J.J., Quast, K.B., Südhof, T.C., Fagiolini, M., and Hensch, T.K. (2009). Common circuit defect of excitatory-inhibitory balance in mouse models of autism. J. Neurodev. Disord. *1*, 172–181.
29. Robertson, C.E., and Baron-Cohen, S. (2017). Sensory perception in autism. Nat. Rev. Neurosci. *18*, 671–684.
30. Robertson, C.E., Kravitz, D.J., Freyberg, J., Baron-Cohen, S., and Baker, C.I. (2013). Tunnel vision: sharper gradient of spatial attention in autism. J. Neurosci. *33*, 6776–6781.
31. Schwarzkopf, D.S., Anderson, E.J., de Haas, B., White, S.J., and Rees, G. (2014). Larger extrastriate population receptive fields in autism spectrum disorders. J. Neurosci. *34*, 2713–2724.
32. Blake, R., Turner, L.M., Smoski, M.J., Pozdol, S.L., and Stone, W.L. (2003). Visual recognition of biological motion is impaired in children with autism. Psychol. Sci. *14*, 151–157.
33. Sutherland, A., and Crewther, D.P. (2010). Magnocellular visual evoked potential delay with high autism spectrum quotient yields a neural mechanism for altered perception. Brain *133*, 2089–2097.
34. Joseph, R.M., Keehn, B., Connolly, C., Wolfe, J.M., and Horowitz, T.S. (2009). Why is visual search superior in autism spectrum disorder? Dev. Sci. *12*, 1083–1096.
35. Flevaris, A.V., and Murray, S.O. (2015). Orientation-specific surround suppression in the primary visual cortex varies as a function of autistic tendency. Front. Hum. Neurosci. *8*, 1017.
36. Gliga, T., Bedford, R., Charman, T., and Johnson, M.H. (2015). Enhanced visual search in infancy predicts emerging autism symptoms. Curr. Biol *25*, 1727–1730.
37. Keehn, B., and Joseph, R.M. (2016). Exploring what's missing: what do target absent trials reveal about autism search superiority? J. Autism Dev. Disord. *46*, 1686–1698.
38. Robertson, C.E., Thomas, C., Kravitz, D.J., Wallace, G.L., Baron-Cohen, S., Martin, A., and Baker, C.I. (2014). Global motion perception deficits in autism are reflected as early as primary visual cortex. Brain *137*, 2588–2599.
39. Tavassoli, T., Hoekstra, R.A., and Baron-Cohen, S. (2014). The Sensory Perception Quotient (SPQ): development and validation of a new sensory questionnaire for adults with and without autism. Mol. Autism *5*, 29.
40. Horder, J., Wilson, C.E., Mendez, M.A., and Murphy, D.G. (2014). Autistic traits and abnormal sensory experiences in adults. J. Autism Dev. Disord. *44*, 1461–1469.
41. Takayama, Y., Hashimoto, R., Tani, M., Kanai, C., Yamada, T., Watanabe, H., Ono, T., Kato, N., and Iwanami, A. (2014). Standardization of the Japanese version of the Glasgow Sensory Questionnaire (GSQ). Res. Autism Spectr. Disord. *8*, 347–353.
42. Mayer, J.L. (2017). The relationship between autistic traits and atypical sensory functioning in neurotypical and ASD adults: a spectrum approach. J. Autism Dev. Disord. *47*, 316–327.
43. Robertson, A.E., and Simmons, D.R. (2013). The relationship between sensory sensitivity and autistic traits in the general population. J. Autism Dev. Disord. *43*, 775–784.
44. Carandini, M., and Heeger, D.J. (2011). Normalization as a canonical neural computation. Nat. Rev. Neurosci. *13*, 51–62.
45. Heeger, D.J., Behrmann, M., and Dinstein, I. (2017). Vision as a beachhead. Biol. Psychiatry *81*, 832–837.
46. Brown, R.J., Candy, T.R., and Norcia, A.M. (1999). Development of rivalry and dichoptic masking in human infants. Invest. Ophthalmol. Vis. Sci. *40*, 3324–3333.
47. Kavšek, M. (2013). Infants' responsiveness to rivalrous gratings. Vision Res. *76*, 50–59.
48. Endo, M., Kaas, J.H., Jain, N., Smith, E.L., 3rd, and Chino, Y. (2000). Binocular cross-orientation suppression in the primary visual cortex (V1) of infant rhesus monkeys. Invest. Ophthalmol. Vis. Sci. *41*, 4022–4031.
49. Zhang, B., Bi, H., Sakai, E., Maruko, I., Zheng, J., Smith, E.L., 3rd, and Chino, Y.M. (2005). Rapid plasticity of binocular connections in developing monkey visual cortex (V1). Proc. Natl. Acad. Sci. USA *102*, 9026–9031.
50. Stedman, A., Taylor, B., Erard, M., Peura, C., and Siegel, M. (2019). Are children severely affected by autism spectrum disorder underrepresented in treatment studies? An analysis of the literature. J. Autism Dev. Disord. *49*, 1378–1390.
51. Tager-Flusberg, H., and Kasari, C. (2013). Minimally verbal school-aged children with autism spectrum disorder: the neglected end of the spectrum. Autism Res. *6*, 468–478.
52. Brainard, D.H. (1997). The Psychophysics Toolbox. Spat. Vis. *10*, 433–436.
53. Oostenveld, R., Fries, P., Maris, E., and Schoffelen, J.-M. (2011). FieldTrip: open source software for advanced analysis of MEG, EEG, and invasive electrophysiological data. Comput. Intell. Neurosci. *2011*, 156869.
54. Bokil, H., Andrews, P., Kulkarni, J.E., Mehta, S., and Mitra, P.P. (2010). Chronux: a platform for analyzing neural signals. J. Neurosci. Methods *192*, 146–151.
55. Baron-Cohen, S., Wheelwright, S., Skinner, R., Martin, J., and Clubley, E. (2001). The autism-spectrum quotient (AQ): evidence from Asperger syndrome/high-functioning autism, males and females, scientists and mathematicians. J. Autism Dev. Disord. *31*, 5–17.
56. Lord, C., Risi, S., Lambrecht, L., Cook, E.H., Jr., Leventhal, B.L., DiLavore, P.C., Pickles, A., and Rutter, M. (2000). The autism diagnostic observation schedule-generic: a standard measure of social and communication deficits associated with the spectrum of autism. J. Autism Dev. Disord. *30*, 205–223.
57. Tang, Y., and Norcia, A.M. (1995). An adaptive filter for steady-state evoked responses. Electroencephalogr. Clin. Neurophysiol. *96*, 268–277.
58. Stanley, J., Forte, J.D., Cavanagh, P., and Carter, O. (2011). Onset rivalry: the initial dominance phase is independent of ongoing perceptual alternations. Front. Hum. Neurosci. *5*, 140.

STAR★METHODS

KEY RESOURCES TABLE

REAGENT or RESOURCE	SOURCE	IDENTIFIER
Deposited Data		
Electrophysiological Data	Mendeley Data	https://doi.org/10.17632/v5ytmfvd7p.1
Software and Algorithms		
MATLAB	Mathworks	http://www.mathworks.com; RRID: SCR_001622
Psychophysics Toolbox	[52]	http://www.psychtoolbox.org; RRID: SCR_002881
FieldTrip Toolbox	[53]	http://www.fieldtriptoolbox.org/; RRID: SCR_004849
Chronux Toolbox	[54]	http://chronux.org; RRID: SCR_005547

LEAD CONTACT AND MATERIALS AVAILABILITY

Further information and requests for resources and reagents should be directed to and will be fulfilled by the Lead Contact, Caroline E. Robertson (caroline.e.robertson@dartmouth.edu). This study did not generate new unique reagents.

EXPERIMENTAL MODEL AND SUBJECT DETAILS

23 adults with autism and 24 control individuals were recruited to participate in this study (Table S1). All participants had normal or corrected-to-normal vision and no history of attention deficit-hyperactivity disorder or epilepsy. All autistic participants met international diagnostic criteria for autism according to the *Diagnostic and Statistical Manual of Mental Disorders*, 4th edition (DSM-IV), as judged by a specialized clinician. Nine participants with autism were being treated with psychiatric medications: antidepressants (n = 9), anticonvulsants (n = 2), stimulants (n = 2), anxiolytics (n = 1). Written consent was obtained from all participants in accordance with the Declaration of Helsinki via a protocol approved by the Massachusetts Institute of Technology Committee on the Use of Humans as Experimental Subjects.

METHOD DETAILS

Psychometric testing

Participants with and without autism were matched for age, gender, and non-verbal IQ, as evaluated using the KBIT-2 (Table S1). All participants also completed the Autism Spectrum Quotient (AQ), a self-report questionnaire that quantifies autistic traits across both autistic and control populations [55]. Additionally, an hour-long diagnostic protocol was administered to all autistic participants (Autism Diagnostic Observation Schedule (ADOS-2) [56]).

Stimuli and Display

Participants viewed a ViewSonic E70fB CRT monitor (width: 15.6 in; resolution: 1280x1024; vertical refresh rate: 160 Hz) from a distance of 30.25 cm (fixed using a chin rest) through a mirror stereoscope. On each trial, two high-contrast checkerboard stimuli were presented (Figures 1A and S1; adapted from [16]) using the Psychophysics Toolbox for MATLAB [52]. Each checkerboard (width: 5.68°) was centered on a black fixation cross and appeared on the horizontal meridian of a yellow screen, one on the left half and one on the right half of the screen. The stereoscope reflected the left/right sides of the monitor into the participants' left/right eyes, so that each eye was presented with only one of the two checkerboards. Fusion was achieved for each participant individually before the experiment began by slowly moving two circles from the edges toward the center of the screen until the participant reported seeing only one circle. All testing took place in a darkened, shielded room.

To independently track the neural response corresponding to each eye during true and stimulated binocular rivalry, we frequency-tagged the two images presented to each eye [16, 17]. Specifically, on each trial, each of the two checkerboard patterns reversed its contrast at a different temporal frequency (5.7 or 8.5 Hz). Across trials, the signature frequency (5.7 or 8.5 Hz) associated with each stimulus/eye was counterbalanced across checkerboards (red or green) and eyes (left or right).

Practice, Rivalry, and Rivalry Simulation Trials

Testing sessions were comprised of three phases: practice trials (two 15 s trials) rivalry trials (three blocks of six 30 s trials) and rivalry simulation control trials (three blocks of six 30 s trials). Each trial was separated by a 15 s break, indicated by a dimming of the screen

background and during which participants were encouraged to blink. At the beginning of each trial, the black circles and fixation crosses appeared on the screen and participants initiated stimulus onset by pressing the "Up" key to start the trial. Throughout both rivalry and simulation trials, participants were asked to continuously indicate whether they perceived "the red image, the green image, or a mixture of the two images" via button press. Before the experiment, participants were given thorough instruction and practice with the task.

In the rivalry condition, a different checkerboard was presented to each eye, one red and one green. In the simulation condition, two identical checkerboards were presented to the two eyes at all times (either red or green). Participants viewed stepwise, sudden transitions between these two concordant images, which alternated on a randomized, timed schedule. The distribution of image durations (mean: 1.9 s) was based on percept durations from a previous rivalry experiment from our lab [1]. These rivalry simulation trials allowed us to measure "ground truth" neural responses to clear, obvious stimulus transitions, to ensure that any differences in neural responses observed during rivalry were not due to baseline differences in neural responses to stimulation at each frequency band. Participants were not informed that they were viewing an alternating stimulus rather than a rivalry stimulus.

EEG Data Acquisition and Pre-processing

Continuous EEG data were acquired using a Biosemi ActiveTwo System from 36 posterior scalp electrodes, digitized at 512 Hz with a lowpass filter at 0.16 Hz and a highpass filter at 100 Hz. EEG data were pre-processed using the MATLAB FieldTrip [53] and Chronux toolboxes (http://www.chronux.org; [54]) and custom MATLAB code. Raw data for each trial was linearly detrended, band-stop filtered at 59-61 Hz, and high-pass filtered at 2Hz. Noisy electrodes were identified using histograms of kurtosis, mean, and variance for each trial, and outlying trials were discarded on a trial-by-trial basis (Controls: 9 total trials; Autism: 3 total trials). Electrodes were re-referenced to the offline common average. SSVEP data were analyzed from the standard 10-20 Oz electrode, which consistently produced high SNRs across all participants.

QUANTIFICATION AND STATISTICAL ANALYSIS

SSVEP Data Analysis: SNR Calculation

To calculate signal-to-noise ratios (SNRs) for each tagged frequency band (5.7 or 8.5 Hz), a Fast Fourier Transform (FFT) was applied to the data for each 30 s trial to extract the trial-averaged amplitudes of the SSVEP response in each tagged frequency band for each participant. Pre-processed EEG data were band-pass filtered ± 2 Hz around our tagging frequencies ([3.7 10.5]) before taking the FFT. SNRs for each tagged frequency band were then calculated as the power at that frequency divided by the mean power in a surrounding band of noise frequencies (+/− 0.5 Hz). EEG data for a given trial was only used in further analyses if the SNR of both tagging frequencies exceeded an SNR threshold of 2. This SNR requirement eliminated five participants from further analyses (Controls: N = 2; Autism: N = 3). Subsequently, the two groups were matched for SNR (Figure S1).

SSVEP Data Analysis: Extracting Response Amplitude Over Time

SSVEP data were subsequently analyzed in three ways. First, to extract the response amplitude in each frequency band as a function of time, data from each time point in the 30 s trial were band-pass filtered ± 0.5 Hz around the desired frequency and analyzed using a Recursive Least-squares (RLS) filter [57]. The first second of each trial was discarded to account for visual transients corresponding to stimulus onset. This analysis step enabled us to track the amplitude of response in each frequency band over time, resulting in an amplitude value for each frequency band (left- and right-eye) at each time point in the 30 s trial.

SSVEP Data Analysis: Antiphase Calculation of Response Amplitude Time courses and Noise Simulations

Second, we used these continuous measurements of response amplitudes (RLS traces) to test whether left- and right-eye frequency bands were antiphase, as would be expected during rivalry. For each rivalry trial, we calculated the antiphase relationship between left- and right-eye frequency bands by calculating the mean phase locking values (PLV) between the two RLS traces for rivalry and simulation trials (where a 0-degree PLV indicates perfectly in-phase signals, and a 180-degree PLV indicates perfectly antiphase signals). Rayleigh's Test was used to determine whether the resulting group PLV distributions were significantly non-uniform for each group (clustered around 180-degrees). To test whether these signals were significantly more antiphase than would be expected by chance, we simulated two noise time courses using randomly shuffled 3 s segments of each participants' own rivalry data for each trial and calculated the resulting PLV magnitudes (averaged over 10,000 iterations / trial).

SSVEP Data Analysis: Neural Rivalry Index Calculation

Third, to quantify the characteristic frequency of each individual's rivalry alternations, we used the continuous measurements of response amplitudes described above to calculate a neural rivalry index (NRI) for each participant. This neural measure of rivalry switch rate is completely naive to the participant's behavioral report. We first computed a "difference time course" for each trial, which represented the difference between the two eyes' RLS traces over the 30 s trial. Specifically, the 5.7 Hz amplitude time course was subtracted from the 8.5 Hz amplitude time course and demeaned. Subsequently, the power spectrum of each difference time course was estimated using the multitaper method (http://www.chronux.org; [54]) (time-bandwidth product TW = 2, and number of tapers K = 3) and averaged across trials. To determine the characteristic frequency of the difference time course from each trial (the participant's NRI), we calculated the half-max of the resulting normalized cumulative distribution function of this trial-averaged power

spectrum. Participants whose NRIs were determined to fall outside of 2 SDs of the group mean were excluded from further analyses (Controls: N = 1; Autism: N = 1).

SSVEP Data Analysis: Intermodulation Frequencies

Previous reports suggest that interactions between the signals from each eye can produce energy at nonlinear intermodulation frequencies, $m * f_1 \pm n * f_2$, when a participant views a mixed percept during rivalry [16, 18]. However, in our study, SSVEP amplitudes in the first intermodulation frequency band predicted neither the duration of mixed states (Controls: p = 0.689; Autism: p = 0.213) nor the proportion of perceptual suppression (Controls: p = 0.138; Autism: p = 0.181), and no significant differences between individuals with and without autism were observed (both p = 0.550). Thus, no subsequent analyses considering intermodulation frequencies were performed.

Support-Vector Machine Analysis: Diagnostic Classification

To determine whether neural data can be used to classify a participant's diagnostic status (autism versus control), we trained and tested a binary support vector machine classifier. Two features were used as inputs to the classifier for each participant: (1) the individual's NRI and (2) the difference between the amplitudes of their tagging frequencies in the FFT of the signal recorded at Oz. In all analyses, the classifier was trained and tested using a linear kernel within a leave-one-participant-out cross-validation scheme. The reported accuracy is an average across the cross-validation folds.

Behavioral Data Analysis

Binocular rivalry analyses were identical to those used in our previously published studies [1, 2]. In brief, participants provided a continuous report of their ongoing perceptual state during each trial via keypress (sampled every 4ms). A sequence of perceptual events was later computed, and perceptual transition was identified whenever one key press was terminated and another began. Two types of transitions were characterized: ''switches'' (e.g., red to mixed to green) and ''reversions'' (e.g., red to mixed to red).

For each trial, the frequency of perceptual switches, as well as the proportion of perceptual suppression were calculated. The proportion of perceptual suppression was calculated as the proportion of each trial spent viewing a fully dominant percept: (dominant percept durations)/(dominant + mixed percept durations). Response latencies during rivalry simulation trials were calculated by comparing the time at which a stimulus appeared on the screen to the timing of the participant's corresponding key press. Anticipatory responses (occurring before trial onset) and response times greater than 2 SDs of the trial mean were removed.

Participants were instructed to initiate each trial by pressing and holding down the up key until they first saw a dominant percept (red or green). This initial keypress corresponding to ''onset rivalry'' [58] was not considered in the analysis. Keypresses lasting < 400 ms and periods where no key was pressed were omitted from the analysis. Participants whose rivalry percept durations were determined to fall outside of 2 SDs of the group mean were excluded from analyses (Controls: N = 2; Autism: N = 1).

DATA AND CODE AVAILABILITY

Original data generated in this study have been published in Mendeley Data and are available at: https://doi.org/10.17632/v5ytmfvd7p.1. Code is available by request to the Lead Contact, Caroline E. Robertson (caroline.e.robertson@dartmouth.edu).

Current Biology, Volume *29*

Supplemental Information

Slower Binocular Rivalry in the Autistic Brain

Alina Spiegel, Jeff Mentch, Amanda J. Haskins, and Caroline E. Robertson

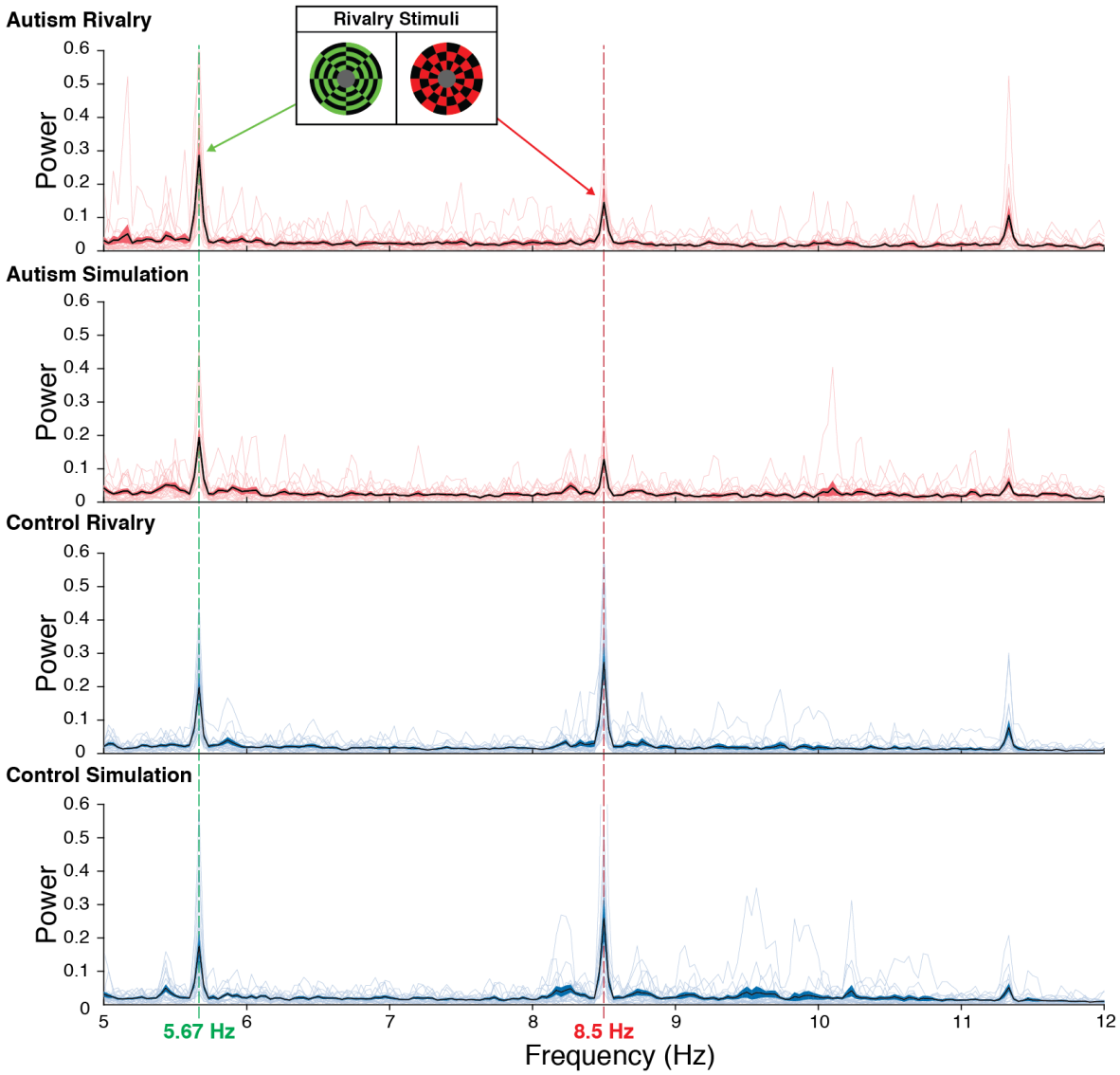

Figure S1. SSVEP technique. Related to Figures 2 and 3. To independently track the amplitude of neural response corresponding to each eye during binocular rivalry, we tagged the two images presented to each eye (green or red checkerboard, top) with a signature frequency (5.67 hz or 8.5 hz). Here, we show the trial-averaged power spectra for each group and condition, with the two tagged frequencies marked in green and red. We observed significant power modulation in each of the tagged frequency bands, which was comparable for the two groups (both $p < 0.001$). No differences were observed in the mean power (dark line) or intrasubject SDs (light shading) of the two groups for either tagged frequency for in either condition (Main Text). Further, SNRs were comparable between the two groups (Main Text).

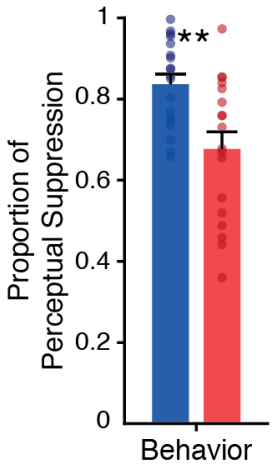

Figure S2. Proportion of Suppression. Related to Figure 2. Individuals with autism reported a reduced proportion of perceptual suppression during rivalry, reporting relatively more period of mixed compared with dominant percepts ($F(1,35) = 11.51$, $\eta_p^2 = 0.248$, $p = 0.002$).

		IQ (Non-verbal)	Age	Gender	ADOS (Com)	ADOS (Social)	ADOS (RRB)	AQ
ASC	N = 18							
	Minimum	82	20		2.00	4.00	0.00	18.00
	Maximum	125	44		6.00	10.00	6.00	46.00
	Mean	108.89	29.83	1.78	3.50	6.89	2.06	32.29
	SD	13.92	7.76	0.43	1.34	1.91	1.63	8.67
Controls	N = 19							
	Minimum	98	18					5.00
	Maximum	132	43					34.00
	Mean	116.89	26.68	1.53				17.18
	SD	9.19	7.04	0.51				7.40
	p-value	0.05	0.21	0.11				0.01

Table S1 Psychometric Data. Related to Figure 1. Groups are matched for age, Non-verbal IQ (KBIT), and Gender (Female = 1; Male = 2). Further, group differences in neural rivalry oscillations and behaviorally-reported rivalry switch rates remained significant when controlling for age and IQ (both $p < 0.017$). Means +/- 1 SEM are shown for each group. *P*-value calculated using two-tailed t-tests.